HHS Public Access

Author manuscript

Comp Biochem Physiol A Mol Integr Physiol. Author manuscript; available in PMC 2024 September 01.

Published in final edited form as:

Comp Biochem Physiol A Mol Integr Physiol. 2023 September ; 283: 111453. doi:10.1016/j.cbpa.2023.111453.

Molecular profiling of CO_2/pH-sensitive neurons in the locus coeruleus of bullfrogs reveals overlapping noradrenergic and glutamatergic cell identity

Lara Amaral-Silva,

Joseph M. Santin*

Division of Biological Sciences, University of Missouri, Columbia, MO, USA

Abstract

Locus coeruleus (LC) neurons regulate breathing by sensing CO_2/pH. Neurons within the vertebrate LC are the main source of norepinephrine within the brain. However, they also use glutamate and GABA for fast neurotransmission. Although the amphibian LC is recognized as a site involved in central chemoreception for the control of breathing, the neurotransmitter phenotype of these neurons is unknown. To address this question, we combined electrophysiology and single-cell quantitative PCR to detect mRNA transcripts that define norepinephrinergic, glutamatergic, and GABAergic phenotypes in LC neurons activated by hypercapnic acidosis (HA) in American bullfrogs. Most LC neurons activated by HA had overlapping expression of noradrenergic and glutamatergic markers but did not show strong support for GABAergic transmission. Genes that encode the pH-sensitive K^+ channel, *TASK2*, and acid-sensing cation channel, *ASIC2*, were most abundant, while *Kir5.1* was present in 1/3 of LC neurons. The abundance of transcripts related to norepinephrine biosynthesis linearly correlated with those involved in pH sensing. These results suggest that noradrenergic neurons in the amphibian LC also use glutamate as a neurotransmitter and that CO_2/pH sensitivity may be transcriptionally coupled to the noradrenergic cell identity.

Graphical abstract

* **Corresponding author**. santinj@missouri.edu.

COMPETING INTERESTS

The authors declare that they have no competing interests.

DECLARATION OF GENERATIVE AI AND AI-ASSISTED TECHNOLOGIES IN THE WRITING PROCESS

The authors declare they did not use AI assisted technologies for writing this manuscript.

SUBMISSION DECLARATION

We confirm that this work is original and has not been published elsewhere, nor is it currently under consideration for publication elsewhere.

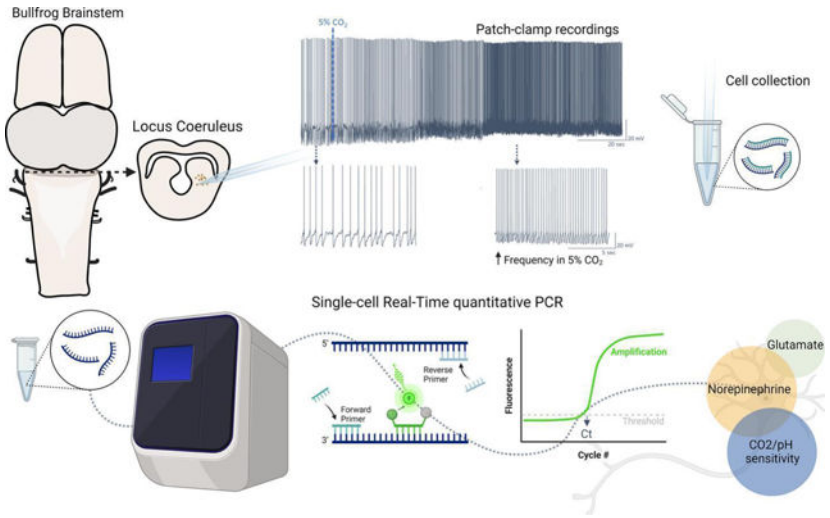

Keywords

Locus coeruleus; neurotransmission; CO_2 chemosensitivity; control of breathing; amphibian

INTRODUCTION

Fast regulation of acid-base balance occurs through adjustments of arterial CO_2 by ventilation. As part of this process, central chemoreceptors play a dominant role in detecting the deviation in CO_2/pH and then signal for corrective changes in ventilation to bring arterial CO_2 back to the set point (Santin, 2018). In recent years the definition of a central chemoreceptor has become increasingly complex. Broadly speaking, central chemoreceptors are neurons or glial cells containing molecules that transduce local changes in acid-base status into neuronal firing or gliotransmitter release to stimulate breathing (Gourine and Dale, 2022; Guyenet and Bayliss, 2015). Several different brain regions contain putative central chemoreceptors, including the retrotrapezoid nucleus (Mulkey et al., 2004), raphé nucleus (Hodges et al., 2008), locus coeruleus (Biancardi et al., 2008), lateral hypothalamus (Dias et al., 2009), the nucleus of the tractus solitarii (Huda et al., 2012), among others. Within these structures, distinct chemosensory molecules have been identified in neurons and glia, such as pH-sensitive ion channels, G-protein coupled receptors (Gestreau et al., 2010; Huda et al., 2012; Kumar et al., 2015; Putnam et al., 2004), CO_2-sensitive connexin hemichannels (Van de Wiel et al., 2020), and HCO_3^- sensitive enzymes and intracellular signaling pathways (Gonçalves and Mulkey, 2018; Imber et al., 2014). Although most of this work has been performed in mammals, the general organization of the central chemosensory system appears to be conserved across vertebrates (Milsom et al., 2022).

A similar view of central chemosensitivity has begun to emerge for amphibians. Indeed, multiple brain regions contribute to the ventilatory response to hypercapnia (Fonseca et al., 2014; Fonseca et al., 2021; Noronha-de-Souza et al., 2006), and neurons appear to act as chemoreceptors (Santin and Hartzler, 2013a). Most of our understanding of central chemoreceptors in amphibians has come from the locus coeruleus (LC), the main source

of norepinephrine (NE) within the brain (Berridge and Waterhouse, 2003; Wang et al., 2022). The LC is required for the increase in "tidal volume" during hypercapnia in anuran amphibians, and focal acidification increases minute ventilation in awake, freely-behaving animals (Noronha-de-Souza et al., 2006). Approximately 85% of the neurons within the LC of frogs enhance their firing rates in response to small increases in CO_2 and may express molecules that give rise to intrinsic CO_2/pH chemosensitivity. Indeed, LC neurons increase membrane resistance during hypercapnia (Santin and Hartzler, 2013a), suggesting the closure of K^+ channels as a potential mechanism of chemosensitivity as occurs in mammals (Li and Putnam, 2013; Pineda and Aghajanian, 1997). In addition, temperature modulates LC neuron firing rates and chemosensitivity (Santin and Hartzler, 2015; Santin et al., 2013), which may control respiratory motor output during temperature changes through noradrenergic signaling (Vallejo et al., 2018). Therefore, neurons within the LC play a major role in ventilatory control of acid-base status in amphibians.

Although the LC is the primary source of NE within the vertebrate CNS, LC neurons also use glutamate and GABA for synaptic transmission. For example, LC neurons co-release NE and glutamate to regulate feeding behavior in mice (Yang et al., 2021). In addition, the mouse LC contains a GABAergic neuronal population that is not noradrenergic to control arousal (Breton-Provencher and Sur, 2019). Moreover, LC neurons of zebrafish are NEergic but co-express either GABAergic or glutamatergic markers (Filippi et al., 2014). Given the heterogeneity of neurotransmitter types within the vertebrate LC, the neurotransmitter profile of chemosensitive neurons in amphibians remains an open question. This has important implications for how activation of LC neurons leads to changes in ventilation (*i.e.*, through relatively slow modulation *via* adrenergic receptors v*s.* fast excitatory or inhibitory transmission onto postsynaptic targets). To address this question here, we determined the neurotransmitter phenotype of LC neurons activated by hypercapnic acidosis (HA) in American bullfrogs. For that, we first performed whole-cell patch clamp recordings to identify LC neurons as putative respiratory chemoreceptors, then harvested these neurons through the patch pipette, and finally performed single-cell quantitative PCR to measure mRNA transcript abundance for markers of NAergic (dopamine beta-hydroxylase; *DBH*), glutamatergic (vesicular glutamate transporter 2; *vGluT2*), and GABAergic transmission (glutamate decarboxylase 1; *GAD1*). In addition, we assessed the overlapping expression of these neurotransmitter genes with mRNA for three candidate pH sensors, the K^+ channels, *TASK2* and *Kir5.1*, and one non-selective cation channel, *ASIC2*. Those channels are recognized to participate in the central chemosensitivity in mammals; *Kir5.1* and *ASIC2* are expressed in the LC, and *TASK2* sense pH in the retrotrapezoid nucleus (D'Adamo et al., 2011; Gestreau et al., 2010; Mir and Jha, 2021). Thus, they provided a reasonable starting point for us to address molecules potentially involved in the CO_2-induced firing response amphibians. This approach allowed us to infer the relationship between neurotransmitter type and potential pH sensors within neurons of LC that respond to CO_2 in adult bullfrogs.

MATERIAL AND METHODS

Animals

The experimental procedure was approved by the Institutional Animal Care and Use Committee at The University of North Carolina at Greensboro (protocol #19–006). The experiments detailed in this study were designed to comply with ARRIVE guidelines and were carried out in accordance with the National Research Council's Guide for the Care and Use of Laboratory Animals. Female Adult American bullfrogs (*Lithobates catesbieanus*) were acquired from Frog Farm (Twin Falls, ID, USA). In the animal facility, the frogs were housed in plastic tanks with access to dechlorinated aerated water and a dry area. The animals were acclimated to lab conditions at 23±2°C in a 12/12 light/dark cycle for at least a week before the experiments. Eight frogs were used in these experiments. The experiments proceed at room temperature 22±1°C.

Dissection and Tissue preparation

Deep anesthesia was achieved by exposing the frogs to 1 ml of isoflurane in a sealed container. After the loss of the toe-pinch reflex, the frog was decapitated, and the head was immersed in 4°C artificial cerebral spinal fluid (aCSF, composition in mM:104 NaCl, 4 KCl, 1.4 $MgCl_2$, 7.5 D-glucose, 1 NaH_2PO_4, 40 $NaHCO_3$, 2.5 $CaCl_2$, all purchased from Fischer Scientific, Waltham, MA, USA). Oxygenation and pH close to values for frogs (~7.85 at ~20°C; (Howell et al., 1970; Reeves, 1972)) were maintained by bubbling the aCSF with 1.5% CO_2 and 98.5% O_2 throughout the brainstem dissection.

Following decapitation, the forebrain was rapidly crushed with forceps, and the skull was quickly removed, exposing the brainstem. The dura was excised, and the brainstem was ventrally glued to a block of agar that was then attached to the vibratome plate using super glue. The midbrain was sliced at 400 μM in cross sections to expose LC neurons (Fournier and Kinkead, 2008; Noronha-de-Souza et al., 2006; Santin and Hartzler, 2013a).

Electrophysiology and single-cell collection

Patch clamp equipment and all the instruments used for patch clamp and cell collection were previously cleaned with a bleach solution, ethanol, and sodium hydroxide solution (RNAse away, Fischer Scientific, Waltham, MA, USA) to record and collect cells in an RNAse-free environment. Midbrain slices were transferred to the recording chamber and stabilized using a nylon grid while constantly perfused with aCSF. Neurons were identified in the area anatomically identified as the LC (González et al., 1994) using 40x magnification (Hamamatsu ORCA Flash 4.0LT sCMOS, Hamamatsu Photonics, Hamamatsu, SZ, Japan). To perform whole cell patch clamp electrophysiology, glass pipettes (2–4 MΩ resistance) were filled with 2.5 μl of a solution containing (in mM) 110-K-gluconate, 2 $MgCl_2$, 10 HEPES, 1 Na_2-ATP, 0.1 Na_2-GTP, and 2.5 EGTA (Fischer Scientific, Waltham, MA, USA). They were then attached to a head stage (CV203BU) and positioned close to neurons using an MP-285 micromanipulator and an MPC-200 controller (all Sutter Instruments, Novato, CA, USA). While approaching the neuron, positive pressure was applied and quickly removed to form a >1GΩ seal. This was then broken for whole cell access using gentle negative pressure applied by mouth.

The chemosensitive response to CO_2 was determined after acquiring stable access in the cell. For that, current clamp was used to monitor tonic firing frequency for 10 minutes to have a stable baseline in aCSF bubbled with standard CO_2 (1.5% CO_2 and 98.5% O_2). The LC neurons had an initial membrane potential of −58.1±5.1mV, and we injected small amounts of positive current prior to stabilization in cells that were not firing tonically. Neurons with membrane potential more positive than −40mV were excluded from the experiment. After achieving stable firing, neurons were exposed to hypercapnia (5% CO_2 and 95% O_2) to elicit an increase in firing frequency (Santin et al., 2013; Santin and Hartzler, 2016). Neurons that presented a clear increase in firing frequency were then collected for molecular analysis, as we previously described (Pellizari et al., 2023). One cell decreased firing in response to CO_2 and was excluded from molecular analysis. After the electrophysiological recordings, we changed the amplifier into voltage clamp configuration, and membrane potential was stepped from – 5 mV to +20 mV at 5 ms intervals to aid in holding RNA in the pipette throughout the cell aspiration (Fuzik et al., 2016). Gentle negative pressure was applied in the glass pipette using a 60 ml syringe while monitoring the seal for 4 minutes. Then negative pressure was progressively increased in the next 3 minutes. Throughout this time, the cell was also visualized through the microscope to ensure that the entire cell was collected and that no other tissue entered the pipette. If we observed debris enter the tip of the pipette, the cell was discarded. The tip of the glass pipette containing the sample was broken in a tube containing 100μl of lysis buffer (Zymo Research, Irvine, CA, USA), and positive pressure was applied to ensure the cell release in the tube. The sample was saved in a −80°C freezer until further analysis. A second group was used as time controls to observe if there would be any spontaneous increase in firing frequency overtime. For this group, we also waited 10 minutes to have a stable baseline as described above (initial membrane potential of −57.1±7.6mV) and maintained the neurons in aCSF bubbled with 1.5% CO_2 and 98.5% O_2 for additional 10 minutes.

Neuronal firing frequency was analyzed as an average of all events within the last thirty seconds in each condition; e.g., control (1.5% CO_2/pH~7.85) and hypercapnia (5% CO_2/pH ~7.35), as well as time control (1.5% CO_2/pH~7.85) at 9.5 min and 19.5 min after entering the whole cell configuration. Analysis was made using the cyclic measurements function on LabChart (ADInstruments, Dunedin, Otago, New Zealand).

Single-cell Real-time quantitative PCR:

Primers and probe design: PCR primers were designed to study a possible noradrenergic (dopamine beta-hydroxylase; *DBH*), glutamatergic (vesicular glutamate transporter 2, *vGluT2*), and GABAergic (glutamate decarboxylase 1; *GAD1*) identity of the neuron. DBH catalyzes the conversion of dopamine to norepinephrine (Weinshenker, 2007). vGluT2 is the most abundant transporter of glutamate into synaptic vesicles in the brainstem (Moechars et al., 2006), and GAD1 catalyzes the decarboxylation of glutamate to GABA (Lee et al., 2019). In addition, we measured the expression of genes with a potential role in pH/CO_2 sensitivity; *KCNK5* that encodes *TASK2*, an alkaline-activated K^+ channel; *ASIC2* that encodes an acid-sensing cation channel subunit; and *KCNJ16* that encodes *Kir 5.1*, a K^+ channel inhibited by acidosis. To identify these sequences, we used the annotated amino acid sequences from *Rana temporaria* as a query in the *Lithobates*

catesbeianus amino acid database, which produced hits for "hypothetical proteins" that had a high amino acid sequence conservation. We confirmed the identity of the hypothetical target protein by performing a reciprocal BLAST against the nonredundant protein database. In all cases, the reciprocal BLAST of the hypothetical bullfrog protein led to a list of sequences that were consistent with the identity of that protein (e.g., a protein we identified as *TASK2* based on homology with *Rana temporaria* always led to a list of *TASK2* from many fish, amphibian, and reptile species when we "reBLASTed." We could not identify *Kir 5.1* sequences in the bullfrog CDS, likely due to low coverage of the *Lithobates catesbieansus* genome (Hammond et al., 2017). Therefore, we used the coding sequence of Kir 5.1 found in *Rana temporaria* (closely related to *L. catesbeianus*). Our rationale was that the close identity of nucleotide sequence between these species would allow us to design primers for use in *Lithobates catesbeianus*.

Once we had the accession numbers, we found the open reading frame in the coding DNA sequence (CDS) to design probe-based qPCR assays using Biosearch Technologies Real Time Design qPCR Design Software. *DBH* and *vGluT2* were grouped into one assay; *TASK2* and *ASIC2* were used in a separate assay, and *GAD1* was run alone. Each assay had forward primers, reverse primers, and a fluorescent nucleotide reporter probe that specific binds to the amplicon of the target PCR product of interest. Thus, probe-based qPCR assays provide specificity at two levels: the primers and probes. All assays were first validated in-house by running a series of four 4-fold dilutions of brainstem cDNA. The only gene that fell below the detection limits of our assay was *DBH*, which was likely diluted out in whole brain homogenates due to highly localized expression within noradrenergic regions. Using the same methodology, we validated the *DBH* assay on the adrenal gland tissue, which is known to have high *DBH* expression (Kobayashi et al., 1994). The primer sets and probes used here are shown in Table 1.

Gene expression measurements: After all cells were collected (n=29) following electrophysiological experiments, the samples were thawed at once, batched processed in parallel, and the steps until gene expression measurement proceeded as we previously described (Pellizzari et al., 2023). Briefly, RNA was extracted and isolated in each single-cell sample using Quick-RNA Microprep kit (Zymo Research, Irvine, CA, USA) according to the manufacturer's instructions. In sequence, we synthesized cDNA using SuperScript IV VILO (Thermo Fisher Scientific, Waltham, MA, USA). We tested the quality of the sample by performing RT qPCR for 18S ribosomal RNA using an SYBR green reaction, following instructions of the 2X SYBR Green Mastermix (ThermoFisher Scientific, Waltham, MA). 18S rRNA was selected as the control gene because ribosomal RNAs represent >80% of the total RNA within a sample and, therefore, provide an estimate of RNA extraction and cDNA synthesis efficiency. Of these 29 neurons, we chose 19 samples that had a threshold cycle (C_t) of ~21 cycles, indicating similar amounts of total RNA in the sample. These 19 neurons then underwent preamplification (PerfeCTa PreAmp SuperMix, Quanta Bio, Beverly, MA, USA) of our target genes by 14 cycles of PCR to enrich these targets within the sample as previously described (Pellizzari et al., 2023).

The samples were then diluted 7.5x In nuclease-free water, and we ran single-cell quantitative PCR on all cells for each of the target genes. For that, qPCR was performed

using 10 μL reactions containing 2.5 μM forward and reverse primers, 312.5 nM reporter probes, and followed the instructions of the 5× PerfeCTa qPCR Toughmix mastermix (Quanta Bio, Beverly, MA, USA). Assays were run on 96-well plates on an Applied Biosystems QuantStudio 6 (Applied Biosystems, Thermo Fisher Scientific, Waltham, MA, USA) using the cycling conditions recommended by the Toughmix mastermix: 50°C–- 2min, 95 °C–- 10 min, 95 °C–- 15 s, 62.5 °C −1 m for 40 cycles of PCR. Conversion of C_t value to an estimation of absolute copy number for each neuron was estimated by interpolating C_t values for each gene into a standard curve of known copy number that was run on the same plate and accounting for the 14 cycles of preamplification (Pellizzari et al., 2023; Santin and Schulz, 2019). Standard curves were generated using gBlock Gene Fragments (IDT Technologies, Coralville, IA, USA) for each amplicon of our target genes and diluting it from 15×10^6 to 150 copies. mRNA copy number for each neuron was then normalized by an "normalization factor" based on 18S Ct values of the population to scale copy number in a way that accounts for potential differences in the efficiency of the cDNA synthesis reaction and starting concentrations within each sample (Schulz et al., 2007).

Data analysis

Statistical analysis—Data are raw values from individual experiments. The effect of hypercapnia or time in control conditions on the firing rate was analyzed using paired t-test. The difference in mRNA abundance among genes involved in neurotransmission or pH sensing was calculated using one-way ANOVA on ranks followed by Dunn's multiple comparison post hoc test. To infer the relationship between neurotransmitter type and potential pH sensors, we performed Pearson correlation. Statistical significance was accepted when $p \leq 0.05$. Nineteen cells from 5 frogs were used in the hypercapnia experiment, followed by qPCR analysis, and 8 cells from 3 frogs were used for time control.

RESULTS:

Amphibian LC neurons increase their firing rates in response to hypercapnic acidosis (Santin and Hartzler, 2013a). However, the neurotransmitter identity of neurons in the LC that are activated by CO_2 is not known. To address this question, we first identified CO_2/pH-sensitivity of neuronal firing in brain slices from adult frogs using whole-cell patch clamp electrophysiology (Fig 1A). All neurons used in this study increased firing rate following exposure to hypercapnia ($p>0.001$, paired t-test), with an average increase of 2.5±1.8 Hz (Fig. 1B-E). To ensure that these responses occurred due to the elevated CO_2 and not a technical issue during the experimental protocol, we performed a separate series of time control experiments. The LC neurons maintained in baseline conditions decreased ~19% of the initial firing rate over 20 min (Fig. S1, change of −0.15±0.16Hz, $p=0.0300$), while the neurons exposed to hypercapnia and used for the molecular analysis increased firing frequency around 288%. These results indicate that the increase in firing frequency in response to hypercapnia was accurate, if not slightly underestimated, in those cells.

Following the whole-cell recording of neurons exposed to hypercapnia each neuron was aspirated into the patch pipette, saved in lysis buffer, and stored at −80°C for qPCR analysis. We then performed absolute quantitative real-time PCR in single LC neurons to

estimate mRNA transcript abundance for markers of neurotransmitter phenotype, as well as candidate pH-sensitive ion channels (Fig 2A). Our data pointed to a strong expression (mRNA abundance) of noradrenergic (*DBH*) and glutamatergic (*vGluT2*) markers, while the GABAergic (*GAD1*) transmission marker was absent from most neurons (Fig 2B). The abundance of neurotransmitter markers differed significantly ($p<0.0001$; Kruskal-Wallis test). Quantitatively, *DBH* and *vGluT2* had similar mRNA copy numbers ($p=0.0857$; Dunn's multiple comparisons test), while both *DHB* and *vGluT2* were significantly greater than *GAD1* (respectively; $p=0.007$ and $p<0.0001$; Dunn's multiple comparisons test). Although these trends reflect the mean data, we note there was variability in the expression of each marker across cells. For example, most neurons expressed *DHB*, but two neurons in the data set had very low levels of *DBH* expression, just on the threshold of detection in our assay. On the other hand, most neurons lacked *GAD1*, but one exhibited a clear signal, suggesting the possibility of GABAergic neurons within the LC as has been shown to occur in mammals (Breton-Provencher and Sur, 2019). Overall, LC neurons activated by HA appear to be noradrenergic and glutamatergic, but distinct cell types may exist in lower frequencies (*i.e.*, only glutamatergic or GABAergic neurons).

pH-sensitive ion channels are thought to be a type of molecule that underlies CO_2/pH chemosensitivity in neurons (Putnam et al., 2004). Therefore, we also measured the expression of three candidate pH-sensitive ion channels, two of which are expressed in the LC of mammals (*Kir5.1* and *ASIC2*), and one with a well-known role in pH sensing of the retrotrapezoid nucleus (*TASK2*) (D'Adamo et al., 2011; Gestreau et al., 2010; Mir and Jha, 2021). All LC neurons expressed *ASIC2* and *TASK2*, while most neurons tended to have lower *Kir5.1* expression (Fig 2C). The copy number varied across channel mRNAs ($p<0.0011$; Kruskal-Wallis test). *TASK2* had similar levels of expression compared to *ASIC2* and *Kir5.1* ($p=0.3820$ and 0.970; Dunn's multiple comparisons test), but *ASIC2* was significantly greater than *Kir5.1* ($p=0.0007$; Dunn's multiple comparisons test). Like the neurotransmitter markers, the general trends in the expression of pH sensors had exceptions. For example, although many neurons had *Kir5.1* expression near or below the detection threshold of our assay, 7 neurons showed expression levels in the range of *TASK2* and *ASIC2*. Therefore, LC neurons responding to HA express the mRNA that codes for several distinct pH-sensitive ion channels, with consistently greater expression of *TASK2* and *ASIC2*.

Neuronal properties (sensory processes, output patterns, synaptic function) are thought to be constrained by genetic mechanisms (Kodama et al., 2020). As a result, multiple physiological processes that define the function of a given cell type are often under the same transcriptional regulatory pathways. This form of control often manifests as mRNA abundances for each process that are regulated at roughly fixed ratios, which manifest as correlations across populations of cells or animals (Goaillard and Marder, 2021; Hu and Santin, 2022; Santin and Schulz, 2019). Thus, genes under shared regulatory pathways often track each other at the mRNA level to give rise to characteristic functions of a given cell type. This led us to test the potential for coupling between the neurotransmitter phenotype and pH sensing in LC neurons.

We found significant correlations between *DBH* vs. *TASK2* (r=0.5488, p=0.0150) and *DBH* vs. *ASIC2* (r=0.6727, p=0.0063) but not *DHB* vs. *Kir5.1* (Fig 3 A-C). In addition, there was a significant correlation between *TASK2* and *ASIC2* (r=0.5526, p=0.0142; Fig 3D). These results indicate that *DBH*, *TASK*, and *ASIC2* all roughly track each other's expression levels across neurons. Interestingly, we did not observe correlations between *vGluT2* and any of the pH-sensitive ion channels (Fig 4A-C), nor did *DBH* correlate with *vGluT2* (Fig 4D). These results indicate that correlated patterns of mRNA expression are specific to norepinephrine biosynthesis and pH sensing channels, at least for this subset of genes. In sum, these data show that LC neurons activated by HA are predominately noradrenergic and glutamatergic, and express pH-sensitive ion channels that covary with *DBH* abundance.

DISCUSSION:

Chemosensitive LC neurons and noradrenergic signaling play a critical role in acid-base regulation through the control of breathing in amphibians (Noronha-de-Souza et al., 2006; Santin and Hartzler, 2013a, b; Vallejo et al., 2018). Although LC neurons are the main source of norepinephrine within the CNS, different vertebrate species contain LC neurons with various neurotransmitter types. Here, we extend previous work by incorporating modern single-cell molecular profiling techniques to define the neurotransmitter profile of CO_2/pH-sensitive LC neurons in bullfrogs. First, we show that most neurons in the LC of amphibians that increase firing rates in response to CO_2 are noradrenergic and glutamatergic. Second, we show that these cells express mRNA that codes for pH-sensitive ion channels. Finally, we observed a linear correlation between mRNA abundance for candidate pH-sensing genes with a noradrenergic identity, which points to a genetic or transcriptional coupling between these processes.

Caveats and limitations

We want to mention important caveats of these data. Most LC neurons of bullfrogs respond to HA and likely play a role in ventilatory response to respiratory acidosis (Santin and Hartzler, 2013a, b; Santin and Hartzler, 2016). However, roughly half of those neurons lose their responsiveness to CO_2/pH when isolated from local networks *via* synaptic blockade, indicating some neurons may respond to HA through synaptic transmission rather than intrinsic CO_2/pH sensing (Santin and Hartzler, 2013a). This is important, as the hypercapnic response by the LC neurons in this study was characterized with synapses and surrounding glia intact. Therefore, even though all neurons included here increased firing rates in response to CO_2, we expect that some may not have been intrinsically chemosensitive, responding via input from synapse (Santin and Hartzler, 2013a) or gliotransmission from astrocytes or microglia. This seems consistent with our data, as we observed a continuum of mRNA abundance for markers of neurotransmitter identity and pH sensing ion channels. We expect that variation mRNA abundances across neurons may correspond with whether neurons are intrinsically chemosensitive.

We also acknowledge the complicated relationship between mRNA and mature protein function. On the one hand, a close matching exists between the expression of genes involved in neurotransmitter biosynthesis and the presence of those enzymes in single

neurons (Marder, 1976; Martinez et al., 2019). Thus, the expression of mRNA transcripts for genes such as *DBH*, *vGluT*, and *GAD* are commonly used to define neurotransmitter phenotypes with molecular profiling techniques (Fremeau Jr et al., 2001; Hartman et al., 1972; Moriyama and Yamamoto, 2004; Pinal and Tobin, 1998). On the other hand, the relationship between ion channel mRNA and the function of those ion channels is not always straightforward. In some cases, mRNA abundance for voltage-gated channels closely tracks the functional measurement of current density across a population of neurons (Schulz et al., 2006). In contrast, the abundance of mRNA for certain ion channels may inversely vary with their functional currents (*e.g.*, when the channel current is large, mRNA abundance is low) (Pellizari et al., 2023; Ransdell et al., 2012). Thus, while we expect pH-sensitive ion channels coded for by these mRNAs to be present in chemosensitive LC neurons, we urge against quantitative arguments about how mRNA relates to the function of these channels and CO_2-induced firing at this time. We view these caveats as important directions for future experiments to understand the molecular organization of central chemoreceptors.

Molecular Profiling of LC Neurons

A major finding of this study is that most LC neurons activated by HA in adult American bullfrogs are both noradrenergic and glutamatergic. In anuran amphibians, noradrenergic fibers project to various parts of the central nervous system, including but not limited to the pallium, cerebellum, olfactory bulb, hypothalamus, as well as those involved in the control of breathing (González et al., 1994; González and Smeets, 1993; Noronha-de-Souza et al., 2006; Smeets and Reiner, 1994). Along with the actions of NEergic signaling on postsynaptic targets, these results suggest that LC neurons likely use glutamate as a neurotransmitter to communicate with these regions. Thus, glutamatergic outflow from the LC may act via a range of receptors, including AMPA receptors, NMDA receptors, and the metabotropic glutamate receptor family. Although the specific mechanistic implications of glutamatergic LC signaling remain to be explored, these results open the possibility for co-transmission of glutamate and NE, as was recently described in mammals (Yang et al., 2021). Although we show clear evidence toward a general trend of glutamatergic and NEergic LC that respond to CO_2, it is important to acknowledge that other cell types did occur in lower frequencies (e.g., a single GABAergic neuron). These data introduce the possibility that LC neurons may also signal through inhibition to regulate breathing. The postsynaptic targets of glutamatergic and GABAergic LC neurons remain to be explored and present an interesting area for future work to understand how chemosensory information within the LC is translated into a ventilatory response.

We also detected mRNA for candidate pH-sensing ion channels in LC neurons. Two of these genes, *Kir5.1* and *ASIC2*, are expressed in the LC of mammals (D'Adamo et al., 2011; Gestreau et al., 2010; Mir and Jha, 2021). Although about one third of neurons expressed *Kir1.5*, the majority did not. However, we identified the expression of *ASIC2* in every neuron. We acknowledge that this channel's half-maximal activation occurs at pH ~4.5 (at least in mammals), which lies far outside the physiological range. However, when combined with other *ASIC* subtypes, the pH sensitivity of *ASIC2* shifts closer to the physiological range, with half-activation values near a pH of 6 and a base of the activation curve near

a pH of 7.5 (Hesselager et al., 2004). In addition, incorporating *ASIC2* into the *ASIC* protein trimer reduces desensitization, preventing channel closure in response to sustained acidosis (Hesselager et al., 2004). Given that LC neurons have high membrane resistance values (0.5–1 GΩ), even slight activation of *ASIC* channels at the base of the activation curve during hypercapnic acidosis to a degree that as we performed here may produce currents of just a few pA to stimulate neurons and increase ventilatory drive (Santin and Hartzler, 2013a). Along with *ASIC2*, each LC neuron analyzed also expressed *TASK2*, one of the critical ion channels for chemosensitivity of the mammalian retrotrapezoid nucleus (RTN) (Gestreau et al., 2010; Kumar et al., 2015). *TASK2* is a K^+ leak channel with a pH sensitivity within the physiological range, being closed by slight acidification and opened by alkalinization (Li et al., 2020). *TASK2* mRNA is strongly expressed in the mammalian RTN and, to our knowledge, has never been detected in the LC. Thus, our data raise the possibility that *TASK2* may play a role in pH sensing in the amphibian LC but was lost in mammals. Expression of multiple pH sensors that operate over different pH ranges is consistent with the broad range of pH values this animal may encounter resulting from temperature changes. For example, K^+ leak channels, including TASK2 and other TASK channels we did not study, may operate as the dominant pH sensors near ~22°C, while *ASICs* may be recruited by respiratory acidosis at higher temperatures when arterial pH is already more acidic (Stinner and Hartzler, 2000); Howell et al., 1970). Future work must address the full profile of pH sensing channels and receptors to understand how animals that regulate variable pH set points to achieve this goal.

Potential coregulation of noradrenergic and pH sensing cell phenotype

Features of neuronal identity are controlled through genetic mechanisms. For example, a matching between firing and neurotransmission is constrained by co-expressing ion channels (Kodama et al., 2020). In addition, genes involved in dopamine metabolism are transcriptionally coupled to the expression of various voltage-gated ion channels in neurons of the substantia nigra (Tapia et al., 2018). Thus, genetic or transcriptional programs integrate multiple cellular properties that define a neuronal type. As these processes are reflected as correlations in mRNA abundance (Goaillard and Marder, 2021), we analyzed our data for correlations between mRNA that codes for neurotransmitter phenotype and pH-sensitive ion channels. We found that the abundance of mRNAs associated with norepinephrine biosynthesis (*DBH*) correlated with both pH sensing channels that were expressed in most neurons (*TASK2* and *ASIC2*). Although *vGluT2* was expressed in these same cells, it did not linearly correlate with any of the pH sensors or *DBH*. Thus, these data suggest that a genetic or transcriptional program links the noradrenergic identity with chemosensitivity, while glutamatergic function may be under separate control mechanisms. We do not yet know the specific mechanisms that maintain mRNAs in the correlated state. Some work indicates that co-expressed genes may be under the control of transcription factors that bind to the same promoter (Veerla and Höglund, 2006). Others have shown that feedback through ongoing activity or neuromodulation maintains mRNA correlations across neurons (Santin and Schulz, 2019; Temporal et al., 2012; Temporal et al., 2014). Regardless of the specific mechanisms, our results introduce the possibility that LC neuron responses to HA are coupled to the noradrenergic phenotype. Thus, a key area for future work will be to address this relationship more comprehensively by determining which gene families

correlate with the noradrenergic phenotype (e.g., additional pH sensing ion channels) and which, if any, correlate with the glutamatergic phenotype (e.g., voltage-gated ion channels or neurotransmission). Overall, these results provide new insights and raise new questions about the molecular organization of central chemoreceptors.

CONCLUSION

In sum, we combined single-cell molecular methods and electrophysiology recording to determine the neurotransmitter phenotype of LC neurons that respond to CO_2 in amphibians. These neurons are both noradrenergic and glutamatergic and express mRNA for at least two pH-sensitive ion channels. Additionally, only the noradrenergic phenotype was correlated to the pH-sensing channels indicating a possible coupling of LC chemoreception to the noradrenergic cell identity in bullfrogs. By integrating single-cell RNA methods and physiology, the present study expands our understanding of the molecular organization of central chemoreceptors in vertebrates.

Supplementary Material

Refer to Web version on PubMed Central for supplementary material.

FUNDING

This work was supported by the National Institutes of (R01NS114514 to JS); and the US Department of Defense (76129-RT-REP to JS).

AVAILABILITY OF DATA AND MATERIALS

All data generated or analyzed during this study are included as individual values in the figures within this published article. Raw data is available in the additional files and from the authors.

Abbreviations

LC	Locus coeruleus
GABA	Gamma-Aminobutyric Acid
PCR	Polymerase Chain Reaction
mRNA	Messenger ribonucleic acid
TASK2	pH-sensitive K^+ channel
ASIC2	Acid-sensing cation channel
Kir5.1	Inwardly rectifying K^+ channel 5.1
DBH	Dopamine beta-hydroxylase
vGluT2	Vesicular glutamate transporter 2

GAD1	Glutamate decarboxylase 1
NE	Norepinephrine
qPCR	Quantitative Polymerase Chain Reaction
RT qPCR	Real-time Quantitative Polymerase Chain Reaction
aCSF	Artificial cerebrospinal fluid
RNAse	Ribonuclease
BLAST	Basic Local Alignment Search Tool
CDS	Coding DNA Sequence
cDNA	Complementary DNA
rRNA	Ribosomal RNA
RTN	retrotrapezoid nucleus

REFERENCES

Berridge CW, Waterhouse BD, 2003. The locus coeruleus–noradrenergic system: modulation of behavioral state and state-dependent cognitive processes. Brain Res Rev 42, 33–84. [PubMed: 12668290]

Biancardi V, Bícego KC, Almeida MC, Gargaglioni LH, 2008. Locus coeruleus noradrenergic neurons and CO_2 drive to breathing. Pflüg Arc Euro J Physiol 455, 1119–1128.

Breton-Provencher V, Sur M, 2019. Active control of arousal by a locus coeruleus GABAergic circuit. Nat Neuro 22, 218–228.

D'Adamo MC, Shang L, Imbrici P, Brown SD, Pessia M, Tucker SJ, 2011. Genetic inactivation of Kcnj16 identifies Kir5. 1 as an important determinant of neuronal PCO_2/pH sensitivity. J Biol Chem 286, 192–198. [PubMed: 21047793]

Dias MB, Li A, Nattie EE, 2009. Antagonism of orexin receptor-1 in the retrotrapezoid nucleus inhibits the ventilatory response to hypercapnia predominantly in wakefulness. J Physiol 587, 2059–2067. [PubMed: 19273574]

Filippi A, Mueller T, Driever W, 2014. vglut2 and gad expression reveal distinct patterns of dual GABAergic versus glutamatergic cotransmitter phenotypes of dopaminergic and noradrenergic neurons in the zebrafish brain. J Comp Neurol 522, 2019–2037. [PubMed: 24374659]

Fonseca EM, Dias MB, Bícego KC, Gargaglioni LH, 2014. Orexin in the toad Rhinella schneideri: The location of orexinergic neurons and the role of orexin in ventilatory responses to hypercarbia and hypoxia. Respir Physiol Neurobiol 224, 90–99. [PubMed: 25434286]

Fonseca EM, Noronha-de-Souza CR, Bicego KC, Branco LG, Gargaglioni LH, 2021. 5-HT neurons of the medullary raphe contribute to respiratory control in toads. Respir Physiol Neurobiol 293, 103717.

Fournier S, Kinkead R, 2008. Role of pontine neurons in central O2 chemoreflex during development in bullfrogs (Lithobates catesbeiana). Neuroscience 155, 983–996. [PubMed: 18590803]

Fremeau RT Jr, Troyer MD, Pahner I, Nygaard GO, Tran CH, Reimer RJ, Bellocchio EE, Fortin D, Storm-Mathisen J, Edwards RH, 2001. The expression of vesicular glutamate transporters defines two classes of excitatory synapse. Neuron 31, 247–260. [PubMed: 11502256]

Fuzik J, Zeisel A, Máté Z, Calvigioni D, Yanagawa Y, Szabó G, Linnarsson S, Harkany T, 2016. Integration of electrophysiological recordings with single-cell RNA-seq data identifies neuronal subtypes. Nat Biotech 34, 175–183.

Gestreau C, Heitzmann D, Thomas J, Dubreuil V, Bandulik S, Reichold M, Bendahhou S, Pierson P, Sterner C, Peyronnet-Roux J, 2010. Task2 potassium channels set central respiratory CO_2 and O_2 sensitivity. PNAS 107, 2325–2330. [PubMed: 20133877]

Goaillard J-M, Marder E, 2021. Ion channel degeneracy, variability, and covariation in neuron and circuit resilience. Annual review of neuroscience 44, 335–357.

Gonçalves CM, Mulkey DK, 2018. Bicarbonate directly modulates activity of chemosensitive neurons in the retrotrapezoid nucleus. J Physiol 596, 4033–4042. [PubMed: 29873079]

González A, Marin O, Tuinhof R, Smeets WJ, 1994. Ontogeny of catecholamine systems in the central nervous system of anuran amphibians: an immunohistochemical study with antibodies against tyrosine hydroxylase and dopamine. J Comp Neurol 346, 63–79. [PubMed: 7962712]

González A, Smeets WJ, 1993. Noradrenaline in the brain of the south african clawed frog Xenopus laevis: A study with antibodies against noradrenaline and dopamine-β-hydroxylase. J Comp Neurol 331, 363–374. [PubMed: 8514914]

Gourine AV, Dale N, 2022. Brain H^+/CO_2 sensing and control by glial cells. Glia 70, 1520–1535. [PubMed: 35102601]

Guyenet PG, Bayliss DA, 2015. Neural Control of Breathing and CO 2 Homeostasis. Neuron 87, 946–961. [PubMed: 26335642]

Hammond SA, Warren RL, Vandervalk BP, Kucuk E, Khan H, Gibb EA, Pandoh P, Kirk H, Zhao Y, Jones M, 2017. The North American bullfrog draft genome provides insight into hormonal regulation of long noncoding RNA. Nat Comm 8, 1433.

Hartman BK, Zide D, Udenfriend S, 1972. The use of dopamine β-hydroxylase as a marker for the central noradrenergic nervous system in rat brain. PNAS 69, 2722–2726. [PubMed: 4560699]

Hesselager M, Timmermann DB, Ahring PK, 2004. pH Dependency and desensitization kinetics of heterologously expressed combinations of acid-sensing ion channel subunits. J Biol Chem 279, 11006–11015. [PubMed: 14701823]

Hodges MR, Tattersall GJ, Harris MB, McEvoy SD, Richerson DN, Deneris ES, Johnson RL, Chen Z-F, Richerson GB, 2008. Defects in breathing and thermoregulation in mice with near-complete absence of central serotonin neurons. J Neurosci 28, 2495–2505. [PubMed: 18322094]

Howell B, Baumgardner F, Bondi K, Rahn H, 1970. Acid-base balance in cold-blooded vertebrates as a function of body temperature. Am J Physiol 218, 600–606. [PubMed: 5412482]

Hu M, Santin JM, 2022. Transformation to ischaemia tolerance of frog brain function corresponds to dynamic changes in mRNA co-expression across metabolic pathways. Proc Roy Soc B 289, 20221131.

Huda R, Pollema-Mays SL, Chang Z, Alheid GF, McCrimmon DR, Martina M, 2012. Acid-sensing ion channels contribute to chemosensitivity of breathing-related neurons of the nucleus of the solitary tract. J Physiol 590, 4761–4775. [PubMed: 22890703]

Imber A, Santin J, Graham C, Putnam R, 2014. A $HCO3^-$-dependent mechanism involving soluble adenylyl cyclase for the activation of Ca^{2+} currents in locus coeruleus neurons. Biochimica et biophysica acta. 1842, 2569–2578 [PubMed: 25092170]

Kobayashi K, Morita S, Mizuguchi T, Sawada H, Yamada K, Nagatsu I, Fujita K, Nagatsu T, 1994. Functional and high level expression of human dopamine beta-hydroxylase in transgenic mice. J Biol Chem 269, 29725–29731. [PubMed: 7961964]

Kodama T, Gittis AH, Shin M, Kelleher K, Kolkman KE, McElvain L, Lam M, Du Lac S, 2020. Graded coexpression of ion channel, neurofilament, and synaptic genes in Fast-Spiking vestibular nucleus neurons. Journal of Neuroscience 40, 496–508. [PubMed: 31719168]

Kumar NN, Velic A, Soliz J, Shi Y, Li K, Wang S, Weaver JL, Sen J, Abbott SB, Lazarenko RMM, 2015. Regulation of breathing by CO2 requires the proton-activated receptor GPR4 in retrotrapezoid nucleus neurons. Science 348, 1255–1260. [PubMed: 26068853]

Li B, Rietmeijer RA, Brohawn SG, 2020. Structural basis for pH gating of the two-pore domain K+ channel TASK2. Nature 586, 457–462. [PubMed: 32999458]

Li K-Y, Putnam RW, 2013. Transient outwardly rectifying A currents are involved in the firing rate response to altered CO_2 in chemosensitive locus coeruleus neurons from neonatal rats. Am J Physiol- Comp Int Reg Physiol 305, R780–R792.

Lee S, Lee Y, Lee G, 2019. The regulation of glutamic acid decarboxylases in GABA neurotransmission in the brain. Archives of Pharmacol Research. 42, 1031–1039.

Marder E, 1976. Cholinergic motor neurones in the stomatogastric system of the lobster. J Physiol 257, 63–86. [PubMed: 181560]

Martinez D, Santin JM, Schulz D, Nadim F, 2019. The differential contribution of pacemaker neurons to synaptic transmission in the pyloric network of the Jonah crab, Cancer borealis. J Neurophysiol 122, 1623–1633. [PubMed: 31411938]

Milsom WK, Gilmour KM, Perry S, Gargaglioni LH, Hedrick MS, Kinkead R, Wang T, 2022. Control of breathing in ectothermic vertebrates. Compreh Physiol 12, 3869–3988.

Mir FA, Jha SK, 2021. Locus coeruleus acid-sensing ion channels modulate sleep–wakefulness and state transition from NREM to REM sleep in the rat. Neurosci Bull 37, 684–700. [PubMed: 33638800]

Moriyama Y, Yamamoto A, 2004. Glutamatergic chemical transmission: look! Here, there, and anywhere. J Biol Chem 135, 155–163.

Moechars D, Weston MC, Leo S, Callaerts-Vegh Z, Goris I, Daneels G, Buist A, Cik M, van der Spek P, Kass S, Meert T, D'Hooge R, Rosenmund C, Hampson RM. 2006 Vesicular glutamate transporter VGLUT2 expression levels control quantal size and neuropathic pain. J Neurosci. 26, 12055–66. [PubMed: 17108179]

Mulkey DK, Stornetta RL, Weston MC, Simmons JR, Parker A, Bayliss DA, Guyenet PG, 2004. Respiratory control by ventral surface chemoreceptor neurons in rats. Nat Neurosci 7, 1360–1369. [PubMed: 15558061]

Noronha-de-Souza CR, Bícego KC, Michel G, Glass ML, Branco LG, Gargaglioni LH, 2006. Locus coeruleus is a central chemoreceptive site in toads. Am J Physiol-Reg, Int Comp Physiol 291, R997–R1006.

Pellizari S, Hu M, Amaral-Silva L, Saunders S, Santin JM, 2023. Neuron populations use variable combinations of short-term feedback mechanisms to stabilize firing rate. PLoS Biology 21(1): e300197.

Pinal CS, Tobin A, 1998. Uniqueness and redundancy in GABA production. Perspectives on developmental neurobiology 5, 109–118. [PubMed: 9777629]

Pineda J, Aghajanian G, 1997. Carbon dioxide regulates the tonic activity of locus coeruleus neurons by modulating a proton-and polyamine-sensitive inward rectifier potassium current. Neuroscience 77, 723–743. [PubMed: 9070748]

Putnam RW, Filosa JA, Ritucci NA, 2004. Cellular mechanisms involved in CO_2 and acid signaling in chemosensitive neurons. Am J Physiol-Cell Physiol 287, C1493–C1526. [PubMed: 15525685]

Ransdell JL, Nair SS, Schulz DJ, 2012. Rapid homeostatic plasticity of intrinsic excitability in a central pattern generator network stabilizes functional neural network output. J Neurosci 32, 9649–9658. [PubMed: 22787050]

Reeves RB, 1972. An imidazole alphastat hypothesis for vertebrate acid-base regulation: tissue carbon dioxide content and body temperature in bullfrogs. Resp Physiol 14, 219–236.

Santin J, Hartzler L, 2013a. Respiratory signaling of locus coeruleus neurons during hypercapnic acidosis in the bullfrog, Lithobates catesbeianus. Resp Physiol Neurobiol 185, 553–561.

Santin JM, 2018. How important is the CO_2 chemoreflex for the control of breathing? Environmental and evolutionary considerations. Comp Biochem Physiol-Part A 215, 6–19.

Santin JM, Hartzler LK, 2015. Activation state of the hyperpolarization-activated current modulates temperature-sensitivity of firing in locus coeruleus neurons from bullfrogs. American Journal of Physiology-Regulatory, Integrative and Comparative Physiology 308, R1045–R1061. [PubMed: 25833936]

Santin JM, Hartzler LK, 2016. Environmentally-induced return to juvenile-like chemosensitivity in the respiratory control system of adult bullfrogs, Lithobates catesbeianus. J Physiolo 594, 6349–6367

Santi JM, Schul DJ, 2019. Membrane voltage is a direct feedback signal that determines ion channel expression patterns in neurons. Curr Biol 20, 1683–1888.

Santin JM, Watters KC, Putnam RW, Hartzler LK, 2013. Temperature influences neuronal activity and CO_2/pH sensitivity of locus coeruleus neurons in the bullfrog, Lithobates catesbeianus. Am J Physiol-Reg, Int Comp Physiol. 305, R1451–R1464.

Schulz DJ, Goaillard J-M, Marder E, 2006. Variable channel expression in identified single and electrically coupled neurons in different animals. Nat Neurosci 9, 356–362. [PubMed: 16444270]

Schulz DJ, Goaillard J-M, Marder EE, 2007. Quantitative expression profiling of identified neurons reveals cell-specific constraints on highly variable levels of gene expression. Proceedings of the National Academy of Sciences 104, 13187–13191.

Smeets WJ, Reiner A, 1994. Phylogeny and development of catecholamine systems in the CNS of vertebrates. Cambridge University Press.

Stinner J, Hartzler LK, 2000. Effect of temperature on pH and electrolyte concentration in air-breathing ectotherms. J Exp Biol 203, 2065–2074. [PubMed: 10851123]

Tapia M, Baudot P, Formisano-Tréziny C, Dufour MA, Temporal S, Lasserre M, Marquèze-Pouey B, Gabert J, Kobayashi K, Goaillard J-M, 2018. Neurotransmitter identity and electrophysiological phenotype are genetically coupled in midbrain dopaminergic neurons. Sci Reports 8, 13637.

Temporal S, Desai M, Khorkova O, Varghese G, Dai A, Schulz DJ, Golowasch J, 2012. Neuromodulation independently determines correlated channel expression and conductance levels in motor neurons of the stomatogastric ganglion. J Neurophysiol 107, 718–727. [PubMed: 21994267]

Temporal S, Lett KM, Schulz DJ, 2014. Activity-dependent feedback regulates correlated ion channel mRNA levels in single identified motor neurons. Curr Biol 24, 1899–1904. [PubMed: 25088555]

Vallejo M, Santin JM, Hartzler LK, 2018. Noradrenergic modulation determines respiratory network activity during temperature changes in the in vitro brainstem of bullfrogs. Respir Physiol Neurobiol 258, 25–31. [PubMed: 30292742]

Van de Wiel J, Meigh L, Bhandare A, Cook J, Nijjar S, Huckstepp R, Dale N, 2020. Connexin26 mediates CO_2-dependent regulation of breathing via glial cells of the medulla oblongata. Comm Bil 3, 521.

Veerla S, Höglund M, 2006. Analysis of promoter regions of co-expressed genes identified by microarray analysis. BMC Bioinformatics 7, 1–15. [PubMed: 16393334]

Wang S, Wang Z, Mu Y, 2022. Locus coeruleus in non-mammalian vertebrates. Brain Sciences 12, 134. [PubMed: 35203898]

Weinshenker D. 2007. Dopamine beta-hydroxylase. In: Enna SJ, Bylund DB, editors. xPharm: the comprehensive pharmacology reference. New York: Elsevier; p. 1–15.

Yang B, Sanches-Padilla J, Kondapalli J, Morison SL, Delpire E, Awatramani R, Surmeier DJ, 2021. Locus coeruleus anchors a trisynaptic circuit controlling fear-induced suppression of feeding. Neuron 109, 823–838. e826. [PubMed: 33476548]

Highlights

- Locus coeruleus (LC) neurons regulate breathing by sensing CO_2/pH in vertebrates.
- In adult frogs, we analyzed the neurotransmitter phenotype of LC neurons and candidate ion channels involved in chemosensitivity using single-cell absolute quantitative PCR.
- Chemosensors expressed markers for noradrenergic and glutamatergic synaptic transmission but not GABAergic synaptic transmission.
- The abundance of mRNA for associated with noradrenaline biosynthesis was linearly correlated with those involved in pH-sensing.

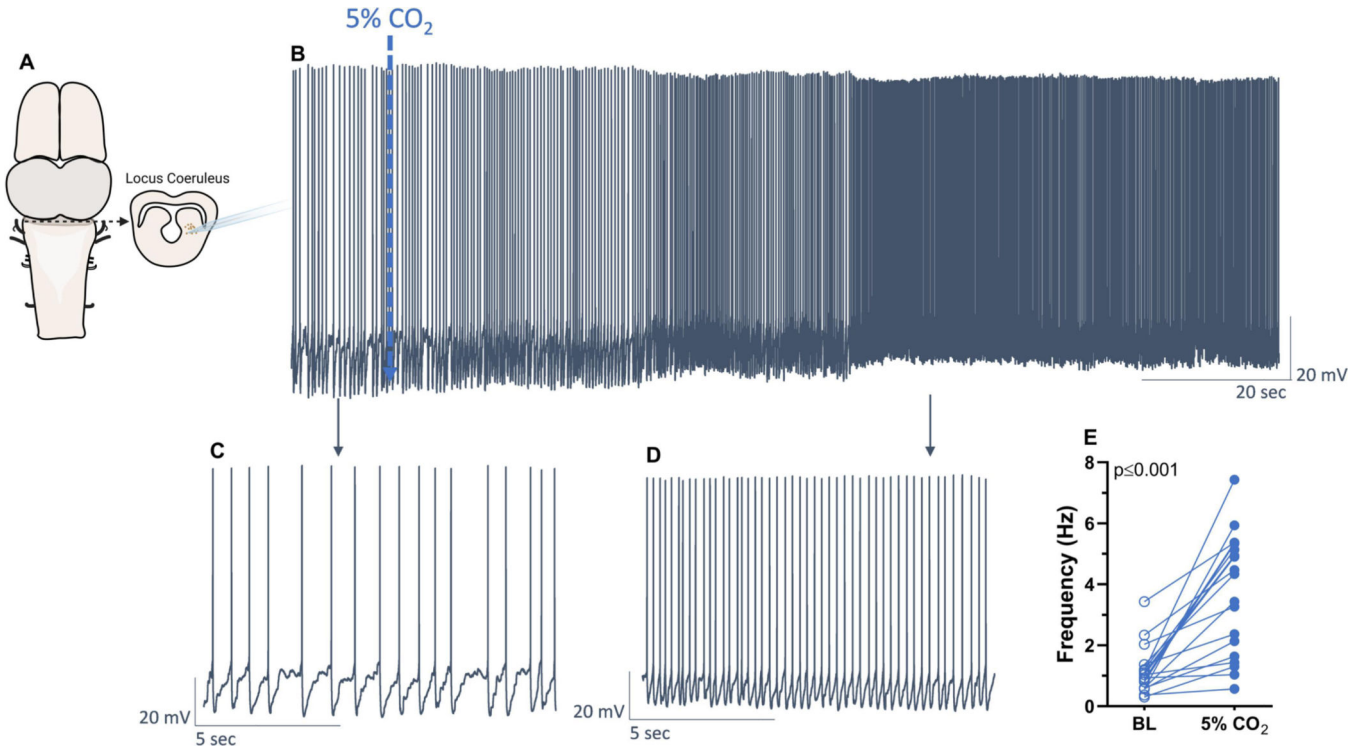

Figure 1 –. Locus coeruleus neurons of adult bullfrogs increased firing frequency in response to hypercapnia (5% CO_2).

Neurons in the region comprising the locus coeruleus (A) had firing frequency recorded in control conditions (B, C) and after being exposed to 5% CO_2 (C, D). Hypercapnia increased firing frequency of all neurons used in this study (E, n=19). Results were compared using paired t-test.

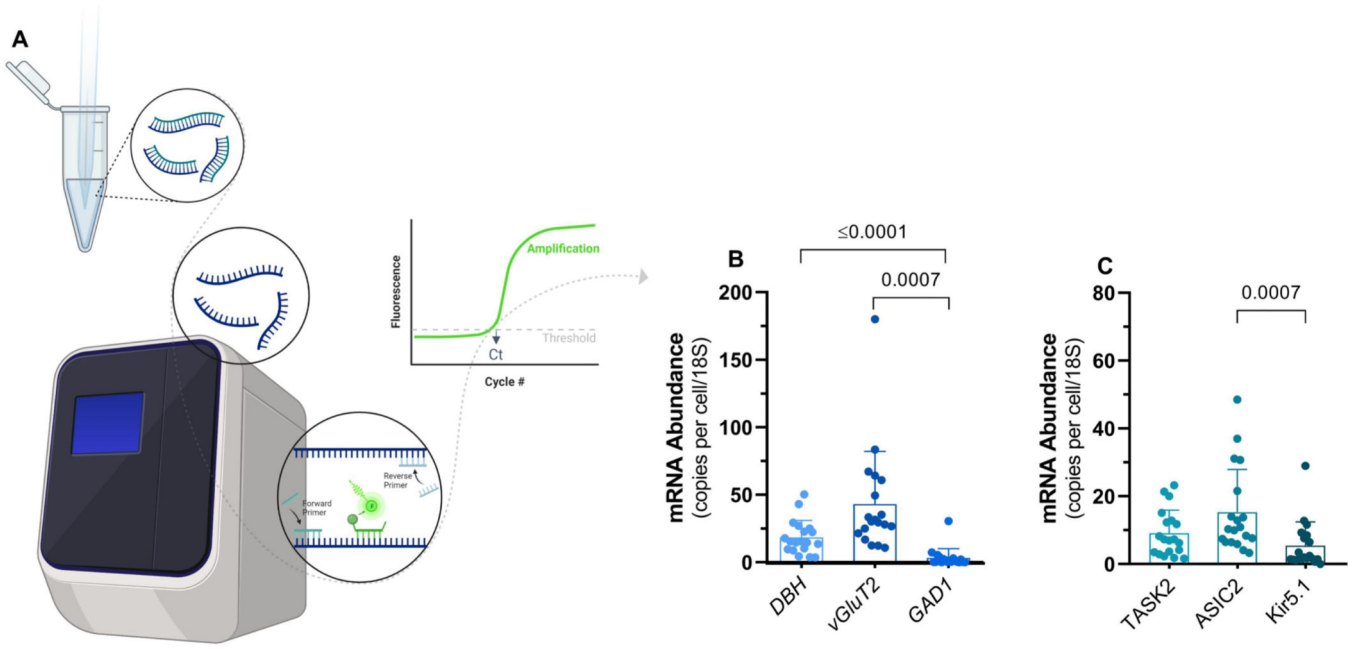

Figure 2 –. mRNA abundance of neurotransmitter markers and candidate pH sensing ion channels.

A) Individual neurons harvested after electrophysiological recordings had gene expression analyzed using RT qPCR (n=19). B) mRNA transcript abundance for markers of noradrenergic (dopamine beta-hydroxylase; *DBH*), glutamatergic (vesicular glutamate transporter 2; *vGluT2*), and GABAergic (glutamate decarboxylase 1; *GAD1*) transmission. C) mRNA transcript abundance for markers of pH sensors, *TASK2* (K+ channel), *ASIC2* (cation channel), and *Kir5.1* (K+ channel). Bars represent means ± SD. Results were compared using one-way ANOVA on rank (Kruskal-Wallis test) followed by Dunn's posthoc tests.

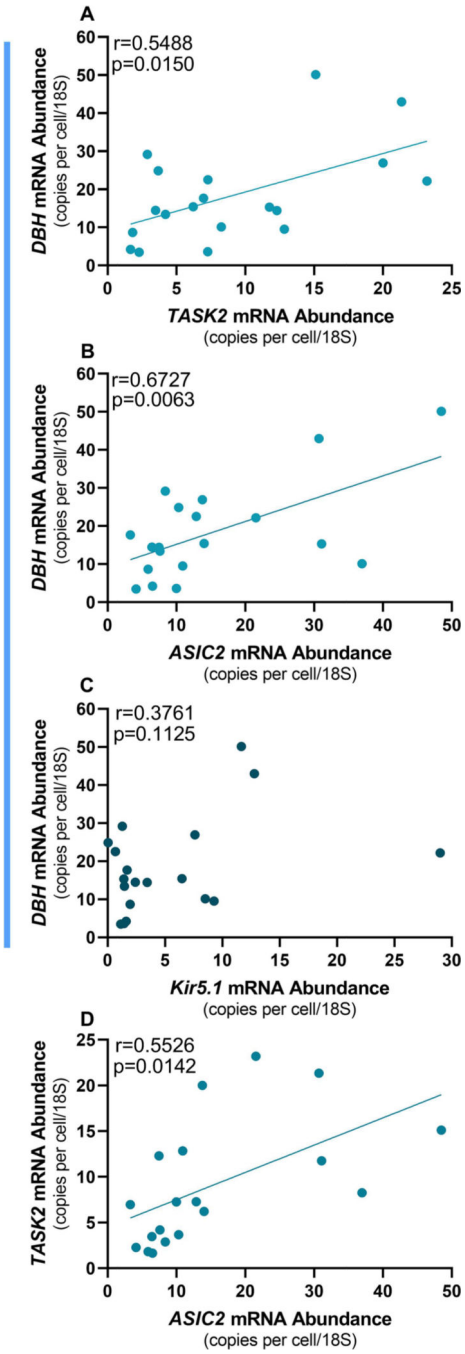

Figure 3. Correlations between the noradrenergic marker (dopamine beta-hydroxylase; *DBH*) and pH sensors

(n=19). Expression of *DBH* was positively correlated to expression of the pH-sensing markers *TASK2* (A) and *ASIC2* (B) but not to *Kir5.1* (C). A positive correlation was also observed between the abundance of *TASK2* and *ASIC2* (D).

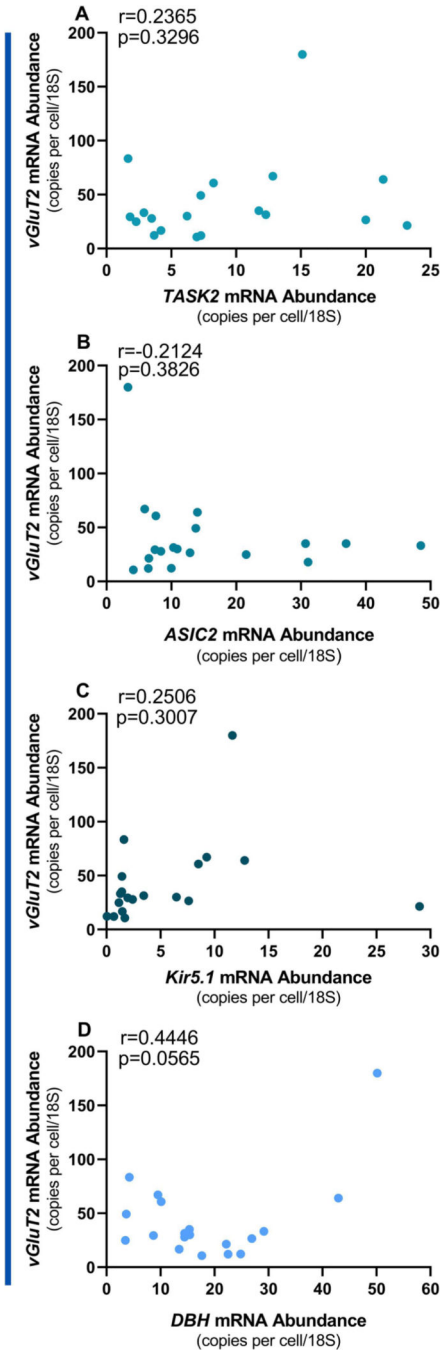

Figure 4. No correlation between the glutamatergic marker (vesicular glutamate transporter 2; *VGluT2*) and pH sensors

(n=19). The expression of *vGluT2* was not related to the expression of the pH-sensing markers TASK2 (A), ASIC2 (B), or Kir5.1 (C). The expression of glutamatergic (*VGluT2)* and noradrenergic (dopamine beta hydroxylase; *DBH*) markers were also not related (D).

Table 1.

Primer sequence for qPCR Assays

Target	Forward Primer	Reverse Primer	Efficiency
DBH	CCGATGATGTCCTGACAATGGA	TCCGTGATGTAGCACCAGTAAG	104%
vGluT2	GATCGTCGGAGCCATGACTAAG	CGGAGGCAAATAAGCCGTAGAAG	102%
GAD1	CAGACCAGGCTCGTTTCCTA	CCGCCCTGGAGATAGTCTTTC	100%
TASK2	CAGGACAAGGAAGCCACGATA	GGTCTCCCAGGGTTCAGATTC	100%
ASIC2	GTGCAGAACCAGCGCTAAG	CAGGGCATTGTACACATGCA	100%
Kir5.1	ACGGCAAACTGTGCCTCATG	CGCACGTTTCCTTCAACAACA	99%

Target	Probe Sequence	Probe-Quencher	NCBI accession # *Lithobates catesbeianus*
DBH	TCTTGCTCCAGATGTTGTCATTCCAGA	FAM-BHQ1a	PIO33490.1
vGluT2	CACGTGAGGAATGGCAATATGTCTTCC	HEX-BHQ1a	PIO31042.1
GAD1	CCACTCTTGCCAGACTAGCCTCCTT	FAM-BHQ1a	PIO41232.1
TASK2	TCATCAACCAATTAGACCGGATCAGTGA	HEX-BHQ1a	PIO29936.1
ASIC2	TTTACTGACAGAGAAGGATGGAGGGTTT	Texas Red-BHQ2a	PIO37540.1
Kir5.1	TGGCGTGTTGGTGACTTTCGAC	FAM-BHQ1a	XM_040331031.1 *

* Kir 5.1 coding sequence was found in Rana temporaria (closely related to L. catesbeianus); see methods.